

# MetaCNV - a consensus approach to infer accurate copy numbers from low coverage data

Stefanie Friedrich (✉ [Stefanie.Friedrich@scilifelab.se](mailto:Stefanie.Friedrich@scilifelab.se))

Stockholms Universitet <https://orcid.org/0000-0002-3889-5589>

Remus Barbulescu

Stockholms Universitet

Thomas Helleday

Karolinska Institutet

Erik LL Sonnhammer

Stockholms Universitet

---

## Software

**Keywords:** Human genome analysis, copy number calling, low coverage data

**Posted Date:** February 4th, 2020

**DOI:** <https://doi.org/10.21203/rs.2.15757/v2>

**License:** © ⓘ This work is licensed under a Creative Commons Attribution 4.0 International License.

[Read Full License](#)

---

**Version of Record:** A version of this preprint was published at BMC Medical Genomics on June 1st, 2020.

See the published version at <https://doi.org/10.1186/s12920-020-00731-y>.

# MetaCNV - a consensus approach to infer accurate copy numbers from low coverage data

Stefanie Friedrich<sup>1</sup>, Remus Barbulescu<sup>1</sup>, Thomas Helleday<sup>2</sup>, Erik LL Sonnhammer<sup>1</sup>

<sup>1</sup> Science for Life Laboratory, Department of Biochemistry and Biophysics, Stockholm University, Box 1031, 17121 Solna, Sweden

<sup>2</sup> Science for Life Laboratory, Department of Oncology-Pathology, Karolinska Institutet, Solna, Sweden

## Abstract

**Background:** The majority of copy number callers requires high read coverage data that is often achieved with elevated material input, which increases the heterogeneity of tissue samples. However, to gain insights into smaller areas within a tissue sample, e.g a cancerous area in a heterogeneous tissue sample, less material is used for sequencing, which results in lower read coverage. Therefore, more focus needs to be put on copy number calling that is sensitive enough for low coverage data.

**Results:** We present MetaCNV, a copy number caller that infers reliable copy numbers for human genomes with a consensus approach. MetaCNV specializes in low coverage data, but also performs well on normal and high coverage data. MetaCNV integrates the results of multiple copy number callers and infers absolute and unbiased copy numbers for the entire genome. MetaCNV is based on a meta-model that bypasses the weaknesses of current calling models while combining the strengths of existing approaches. Here we apply MetaCNV based on ReadDepth, SVDetect, and CNVnator to real and simulated datasets in order to demonstrate how the approach improves copy number calling.

**Conclusions:** MetaCNV, available at <https://bitbucket.org/sonnhammergroup/metacnv>, provides accurate copy number prediction on low coverage data and performs well on high coverage data.

28 **Keywords:** Human genome analysis, copy number calling, low coverage data

## 29 **Background**

30 An important aspect of genome analysis is the study of genetic alterations between individuals in a  
31 cohort, or between samples from one individual, for instance to understand cancer progression. One  
32 type of genetic alteration is copy number variation (CNV), which describes the fact that a segment of  
33 a genome, for example spanning one or more genes, is amplified or deleted.

34

35 Up to 10% of the human genome has been estimated to contribute to CNVs, and abnormal copy  
36 numbers have been linked to mutation-prone diseases like cancer [1]. Knowledge about CNVs is not  
37 only crucial to understanding such diseases, especially with regards to their evolution, but also their  
38 effects on various phenotypes.

39

40 Next-generation sequencing has revolutionized the possibilities to study inter- and intra-individual  
41 genome alterations. For accurate CNV analysis, typically tissue samples with 200-500 ng of DNA are  
42 required for sequencing with high coverage [2]. However, new generations of sequencing techniques  
43 arise and new approaches to sequence even single cell genomes are being developed that only require  
44 50 ng of DNA [2–4]. Copy number callers applicable to sequenced samples with very small amounts  
45 of DNA would create the possibility to investigate CNVs of smaller areas within a larger tissue  
46 sample, such as regions microdissected by laser, and thus offer spatial information of CNVs within  
47 formerly bulk-sequenced samples.

48

49 CNVs can be detected experimentally with various assays, such as [comparative genomic](#)  
50 [hybridization \(CGH, e.g. bacterial artificial chromosomes \(BAC\) array\)](#), fluorescent in situ  
51 [hybridization \(FISH\)](#), and [genotyping array](#). Another option is calling CNVs from genome sequences,

52 although calling correct copy numbers this way is a challenging task. To develop a solution, four  
53 different approaches have emerged, each built on certain assumptions and each with advantages and  
54 disadvantages. [5, 6]

55

56 Callers purely based on a read coverage approach (i) predict copy number changes using the read  
57 coverage of a segment of the genome relative to the coverage of the whole genome. To achieve good  
58 results for both deletions and amplifications, this approach requires high sequencing depth (Figure S1).  
59 Further, short CNVs are often missed. The majority of existing copy number callers apply this  
60 concept, for example ReadDepth [7], CNV-seq [8], cn.MOPS [9], Control-FREEC [10], and  
61 CNVnator [11].

62

63 Callers based on a paired-end mapping, also termed read-pair, approach (ii) predict copy numbers  
64 based on changes in the insert size of paired-end reads. This approach requires paired-end sequenced  
65 data and only considers those pairs of reads where both ends of a pair, i.e. concordantly, have been  
66 mapped. This decreases the number of reads and thus the amount of data that can be used for copy  
67 number calling. Further, the detectable deletions and amplifications depend on the given insert size of  
68 the concordantly mapped read-pair [12]. With a paired-end mapping approach, amplifications larger  
69 than the insert size cannot be discovered. However, the paired-end mapping approach is relatively  
70 independent from the sequencing depth. Further, this approach is appropriate to identify structural  
71 variants in general (e.g. inversions, inter and intra-chromosomal translocations) [5, 13]. A popular  
72 package is BreakDancer [14].

73

74 The split-reads approach (iii) takes only discordant mapped reads; that is, only one mate was aligned  
75 concordantly. For the unmapped read, alignment to a reference genome is reattempted by splitting the  
76 read and aligning both parts separately. A popular package doing this is PINDEL [15].

77 Callers that apply combinations of the above described approaches, i.e. hybrids, represent the fourth  
78 type (iv). Combining a paired-end read and a read depth approach seems to be the most beneficial [5],  
79 for instance used by the callers SVDetect [16] and CNVer [17].

80

81 The rapidly growing field of single cell DNA (scDNA) sequencing challenges calling of variants, e.g.  
82 copy numbers, for individual cells having coverages  $\sim 1x$ . Examples of such callers specified for  
83 scDNA are Ginkgo [18] and SCNV [19]. They are both based on a read depth approach and correct  
84 for GC content bias. A limitation with these methods is that in order to deal with technical artefacts  
85 introduced by single cell sequencing leading to high noise, they require pools of at least 3 cells for  
86 calibration or normalisation. SCNV is further an example of adapting an established bulk method,  
87 SeqCBS, to scDNA data [19]. Another method is Lumpy [20], a structural variant caller applicable to  
88 low coverage data. However, it only outputs cnv types, i.e. deletion or amplification.

89

90 However, in general callers require relatively high sequence coverage to achieve good results, or if  
91 specialised in scDNA, callers require multiple cells to be applied on. [Although higher sequencing](#)  
92 [depth can be achieved with technologies like polymerase chain reaction \(PCR\), this leads to unevenly](#)  
93 [distributed copies of unique molecules, and fewer unique molecules with increasing sequencing depth](#)  
94 [influencing mutation calling](#). We here introduce MetaCNV, a method that combines different  
95 approaches in order to create a caller that is sensitive enough to detect CNVs in low coverage data  
96 [\(below 10x\)](#), even one single cell, but also works on [normal and higher coverage data \(above 30x and](#)  
97 [100x, respectively\)](#). It is a generally applicable method that in contrast to previous low coverage  
98 methods can be applied to single samples.

## 99 **Algorithm and Implementation**

### 100 **Implementation**

101 MetaCNV v1.4 is intended for use on unix operating systems. The graphical user interface was  
102 created with the GTK+ toolkit, a free library available for the majority of current unix distributions.

### 103 **MetaCNV algorithm**

104 MetaCNV combines the prediction of copy number callers based on different approaches and builds a  
105 consensus to achieve higher prediction accurateness. Some copy number callers (e.g. SVDetect)  
106 require a matched sample, for example to be able to distinguish somatic (only detected in the primary  
107 sample) from germline mutations (also found in the matched sample, e.g. blood). One of the current  
108 input callers for MetaCNV, SVDetect, was run with three different matched sample versions: a  
109 matched blood sample, a simulated normal sample with 20x read coverage, and a simulated null  
110 (simNull) alignment with constant zero read coverage, to test if this choice affects the prediction  
111 accurateness and increases sensitivity especially on low coverage data.

112

113 Running MetaCNV comprises five steps (Figure 1).

114

### 115 **Choice of current input callers**

116 The current input callers for MetaCNV were chosen due to their relatively good prediction  
117 accurateness on low coverage data (Figures 4 & S13). Further, they belong to different calling  
118 approaches which perform differently depending on the type of a CNV. In low coverage data, we  
119 observed that ReadDepth v0.9.8, which applies a read depth approach, predicts mid-sized ( $10^6$ - $10^8$  bp)  
120 and larger deleted segments ( $>10^8$  bp) more accurately than other callers, whereas amplifications were  
121 more accurately predicted by SVDetect v1.3, a representative of the hybrid approach.

122

123 Finally, a caller's prediction coverage (Figure S7A, Table S3) is considered. Only ReadDepth and  
124 CopyCat [21] predict gapfree CNVs for an entire genome. Gapfree means that for each base pair of an  
125 investigated genome, a copy number is calculated which resulted in a high prediction coverage.  
126 SVDetect predicted for more than 90% of the genomes. The prediction coverage of Control-FREEC  
127 and CNVnator varied [in cancer cell data sets](#) from 33 to 65% and 35 to 80%, respectively.  
128 ReadDepth is built on the coverage-based approach, predicting copy numbers gapfree for the whole  
129 genome. It applies a negative binomial distribution to approximate an overdispersed Poisson  
130 distribution [7]. Further, it outputs absolute copy numbers for equally-sized, non-overlapping bins  
131 (Table S15). The optimal bin size is calculated by ReadDepth, but can be indirectly adapted by  
132 changing the false discovery rate.

133

134 SVDetect is a tool used to detect general structural variants and is based on the hybrid approach for  
135 copy number calling, meaning both the coverage and any change in the insert size of read-pairs are  
136 considered when inferring copy numbers [16]. SVDetect copy numbers are not predicted gapfree, and  
137 in contrast to ReadDepth and CNVnator it requires for copy number calling a matched normal sample  
138 with which to relate the studied sample (Table S16).

139

140 CNVnator [v0.3.2](#), like ReadDepth, is based on the coverage approach, but with an additional mean-  
141 shift approach that produces a probability distribution function from the coverage data, and links each  
142 data point, i.e. bin, to its maxima. Further, CNVnator is calibrated using the extensive validation done  
143 by the 1000 Genomes Project [11, 22]. Similar to SVDetect, it does not calculate copy numbers for  
144 the entire genome. As with SVDetect, the bin size can be modified by the user. Despite achieving  
145 good prediction accurateness on high coverage data, CNVnator predicts extremely high copy numbers  
146 on low coverage data (Figures S8, Table S17). However, it still produced reliable classification of  
147 segments into deletions and amplifications for low coverage data as accurately as SVDetect and

148 ReadDepth, and complements their predictions (Figure S13, Table S17). Based on this, ReadDepth,  
149 SVDetect, in combination with CNVnator as a referee for conflicts between ReadDepth and SVDetect  
150 were chosen as input callers for MetaCNV.

### 151 **Matched sample in SVDetect**

152 When SVDetect was run as part of MetaCNV, a simulated null sample with zero read coverage  
153 (simNull) was used. The simNull alignment as matched sample is a novel idea to increase sensitivity  
154 and to remove an additional source of noise for low coverage data. If comparing a low coverage  
155 sample with a matched sample having high coverage it will disturb a correct copy number calling.  
156 Ideally, a matched sample should have the same constant coverage as the sample to investigate. With  
157 current tools this constant coverage on each base pair of the genome is not achievable (Figure S21).  
158 Therefore, we developed the novel idea of a simulated null alignment containing zero coverage, and  
159 thus no noise.

160  
161 When SVDetect was run outside of MetaCNV for comparison, two different types of such matched  
162 samples were tested: a matched normal sample (matchedNormal) and a simulated normal sample with  
163 constant read coverage (simNormal).

164  
165 The matched normal was taken from the cancer cell lines HCC1187 and HCC2218 (Table 1) for  
166 which such samples are available (blood samples HCC1187BL and HCC2218BL). The simulated  
167 normal was inferred using Pirs [23].

### 168 **Segmentation of the genome**

169 ReadDepth divides a given genome into bins of a calculated minimum or a multiple of the minimum  
170 bin size. The bin size can only be manipulated indirectly by increasing the false discovery rate. For  
171 both, the high and low coverage study of sequenced single cells, it was set to 0.01 (default). SVDetect  
172 accepts a bin size given by the user. Several bin sizes were tested for SVDetect but the best results

173 were achieved with a bin size of 400 bp and no bin overlap. Based on the calculated bin sizes from  
174 both callers hidden in the start and end position in the output files, new bins were calculated with  
175 different sizes while also considering all breakpoints given by the input callers (Figure 2). At the end  
176 of the MetaCNV prediction process, bins with a similar copy number to one decimal place were  
177 merged into one segment.

## 178 **MetaCNV model**

179 The MetaCNV model contains rules to be applied to each bin, depending on the predicted copy  
180 numbers of the input callers representing different approaches of copy number calling; the strength of  
181 rules is in the decreased risk of overfitting. In general, MetaCNV accepts deletions and normal copy  
182 numbers if they are predicted by a coverage approach (current ReadDepth), and amplifications if they  
183 are predicted by a read-pair approach or hybrid approach of coverage and read-pair (current  
184 SVDetect). More detailed rule descriptions are listed in Table S18. To distinguish between deletions  
185 and normal copy numbers from amplifications, two thresholds  $T1$  and  $T2$  are introduced.  $T2$  is the  
186 local minimum of the frequency of copy numbers produced by ReadDepth between 2 and 2.3; the  
187 other threshold  $T1$  is calculated as  $2 * P - T2$  where  $P$  is the ploidy value (Figure 3).

188 Due to gaps in the predictions from at least one current input caller (no copy number predicted) or  
189 conflicting predicted copy numbers from both callers, the MetaCNV model comprises additional rules  
190 and includes CNVnator as the referee in such conflicting cases.

## 191 **Normalisation of input data**

192 When developing a consensus approach, the results of the considered input callers need to be  
193 normalised in order to compare their results correctly. The detected bias in the predicted copy  
194 numbers of each input caller was corrected with a copy-number-dependent normalisation. The bias  
195 (systematic error) is the difference between frequency peak and ploidy (Figure 3, equations 1), where  
196 CN is the predicted copy number by a caller,  $CN_{norm}$  is the normalised CN, and  $P$  is the ploidy value  
197 which is for the autosomes 2 and for the allosomes either 2 if female or 1 if male. The maximum  
198 absolute bias correction is 0.5.

199  $CN_{norm} = CN + (factor \times bias)$  (1)

200  $bias = P - CN \text{ at } \max(\text{frequency}(CN))$  (1a)

201  $factor = \min\left(\frac{1}{2} \times CN ; 1\right)$  (1b)

202 **Converting log2 values into absolute copy numbers**

203 In general, callers predict copy numbers either as absolute copy numbers or as log ratio values which  
 204 can be converted into absolute copy numbers with

205  $CN_{corrected} = P \times 2^{CN_{log2,corrected}}$  (2)

206 Absolute copy numbers reflect the number of repeats of the sequence [7]. The log<sub>2</sub> values represent  
 207 log<sub>2</sub> transformed ratios to a matched sample or the ploidy *P* [6].

208 When MetaCNV is run with input from SVDetect using a simulated normal sample, the  
 209 formula above (equation 2) is applied to convert log<sub>2</sub> values into absolute copy numbers for  
 210 each bin. Before this, the log<sub>2</sub> values  $CN_{log2}$  are corrected with a genome wide median:

211  $CN_{log2,corrected} = CN_{log2} - \text{median}(CN_{log2})$  (2a)

212 When MetaCNV is run with input from SVDetect using a simulated null alignment, the predicted  
 213 values are accepted as copy numbers. This produces  $CN_{log2}$  values that are always non-negative,  
 214 because in the case of the simulated null alignment, they are relative to 0. Further, a distortion was  
 215 observed which increases exponentially with the true amplification. This distortion is corrected with  
 216 an equalizer factor *q* (Figure 20, equation 3). The net effect corresponds to a back log transformation  
 217 that is calibrated to result in absolute copy numbers.

218  $CN_{meta} = CN_{log2} \times q$  (3)

219  $q = \left(1 + \frac{1}{100} \times CN_{log2}\right)^{0.75 \times CN_{log2}}$  (3a)

## 220 **Calculating error scores**

221 Each MetaCNV bin is annotated with an error score  $e$  mirroring the prediction similarity of the input  
222 callers. The score depends on the consensus of the input callers per bin and is averaged for the  
223 optimised segments considering the bin length per segment. The error score per bin is calculated as  
224 the squared absolute copy number difference between ReadDepth and SVDetect:

$$225 \quad e_{bin} = (CN_{RD} - CN_{SVDetect})^2 \quad (4)$$

226 For bins where ReadDepth did not predict a copy number, we assume  $CN = 0$ . ReadDepth predicts  
227 copy numbers gapless for a genome. Although, rare large gaps happen to occur but they are caused by  
228 non-sequenced regions which not contain genetic regions according to the reference genome GRCh38  
229 [30]. If SVDetect did not predict a copy number,  $CN = P$  is used. SVDetect does not predict copy  
230 numbers gapless for a genome although the coverage is sufficient in case of the high coverage data  
231 and no other obvious reason could be identified. (Pre-processing and application of calling methods,  
232 Suppl.)

## 233 **Accurateness evaluation**

234 To evaluate the accurateness of a caller, its result needs to be compared to true copy number  
235 variations. Different ways were taken to set such a gold standard: simulated data, for example for the  
236 validation of CNV-seq; clinical data with experimentally confirmed CNV, e.g. for the validation of  
237 CNVnator; or cancer cell lines, e.g. for the validation of Control-FREEC and ReadDepth.

238

239 Further, the comparison between true and predicted copy number has either been performed for  
240 segments, e.g. validation of Control-FREEC and ReadDepth, or for genes [24]. Different accurateness  
241 measures have been applied, including accuracy, false discovery rate, F1-score [25], receiver  
242 operating characteristic with true positive and false positive rates [26], Spearman correlation, and root  
243 mean squared error [27].

244

245 Finally, absolute copy numbers,  $\log_2$  ratio values or the class of a copy number [25], which is either a  
246 deletion or an amplification, were considered. Absolute copy numbers are decimal or integer values  
247 mirroring the number of repeats of the sequence [7] whereas the  $\log_2$  ratios stand for log transformed  
248 ratios to a matched sample or the ploidy [6].

249  
250 The prediction accurateness of a regression model, which is the case if comparing copy numbers, can  
251 be evaluated using the mean squared error (MSE, equation 5) and mean absolute error (MAE). In  
252 general, an error based measure calculates the difference between a true and a predicted value, which  
253 in this case is the difference between true and predicted copy number per gene. The mean absolute  
254 error presents the average error, whereas the mean squared error combines systematic and random  
255 error into one value [28]. It also penalizes outliers: each distance is squared, and larger distances thus  
256 get more weight.

257  
258 The true copy number per gene,  $x_i$ , was compared with the predicted one,  $\hat{x}_i$ , by calculating the  
259 residuals  $x_i - \hat{x}_i$  for all genes  $N$ .

$$\text{Mean squared error } MSE = \frac{1}{N} \sum_{i=1}^N (x_i - \hat{x}_i)^2 \quad (5)$$

260  
261 To avoid outlier penalty we compare additionally the prediction accurateness with the mean log ratio  
262 error:

$$\text{Mean log ratio error } MLRE = \frac{1}{N} \sum_{i=1}^N LR, \quad LR = \text{abs} \left( \ln \frac{x_i + 1}{\hat{x}_i + 1} \right) \quad (6)$$

263  
264 If a caller predicts highly different copy numbers for genes of a genome having the same true copy  
265 number but also predicts similar copy numbers for genes with different true copy numbers, then the  
266 analysis of copy number variations can become difficult. Therefore, copy number callers were also  
267 evaluated by the variance of the residuals, which mirrors how close the predicted values surround

268 each unique true copy number (equation 7. For each unique true copy number (integer) value, the  
269 variance of the predicted values was calculated, however, default elements were replaced with the  
270 residuals  $z_i$  (the difference between actual  $x_i$  and predicted value  $\hat{x}_i$ ). The variances are then averaged  
271 for the total number of unique true copy numbers  $M$ .

$$\text{Variance of residuals } \sigma_{Res}^2 = \frac{1}{M} \sum_{j=1}^M \left( \frac{1}{N} \sum_{i=1}^N (z_i - \bar{z})^2 \right) \quad (7)$$

272  
273 Matthew's correlation coefficient (MCC) [29] can be applied for classification models and is  
274 especially applicable for unbalanced ratios of the four confusion matrix categories, which is the case  
275 for the cancer cell lines used in this paper (ratio of amplified/deleted genes from 0.8 to 5, Table 1). To  
276 define the classes of deletions and amplifications for ploidy  $P = 2$ , copy numbers  $> 2.75$  were set as  
277 amplifications and copy numbers  $< 1.75$  were set as deletions, while values in between were set as  
278 normal. In order to deal with these three classes (deletion, normal, amplification), the values for true  
279 positives, true negatives, false positives and false negatives were micro-averaged. This means that for  
280 example the true positive value  $TP$  is equal to  $TP_{class1} + TP_{class2} + TP_{class3}$ .

281  
282 The prediction accurateness of several copy number callers and MetaCNV was evaluated using  
283 known amplified or deleted genes that were publicly available along with well-studied cancer cell  
284 lines. MetaCNV was developed for low coverage data. Therefore, MetaCNV's accurateness was  
285 verified on single sequenced cells of a cancer cell line (SKBR3) having 1x to 6x read coverage.  
286 Additionally, the accurateness was assessed on four cancer cell lines with normal and high coverage  
287 (62x to 104x coverage, Table 1). The range of copy numbers among the cancer cell lines was limited.  
288 To validate MetaCNV on a wider range of copy numbers and also genome-wide, mutated genomes of  
289 different coverages were simulated. MetaCNV's accurateness was compared with other callers'  
290 accurateness by MLRE and MCC (MSE, MAE, and Spearman's correlation in Figures S11, S13, S14).  
291

292 For each caller, we map the output (segments and corresponding copy numbers) per cancer cell line  
293 and simulated genome to the human assembly GRCh38 Ensembl (release 84) [30]. Due to different  
294 segment sizes, this mapping resulted in one or several predicted copy numbers per gene. In such cases,  
295 the total copy number per gene was the sum of the weighted copy numbers, depending on their  
296 segment length within the gene (Figure S9). There were gaps in the prediction of SVDetect,  
297 CNVnator, and Control-FREEC, that is, no copy number for a segment was called. Such gaps within a  
298 gene were filled using the ploidy value. Some segments of the cancer cell lines given by COSMIC [31]  
299 (Cosmic, Suppl.) did not cover a gene completely. In these rare cases, the gene was reduced to the  
300 covered segment length within this gene.

### 301 **Cancer cell lines**

302 Cancer cell lines, like the HeLa cancer cell line, which can theoretically be divided and replicated  
303 indefinitely, contain cells taken from e.g. naturally-occurring cancer tissues [32]. They are publicly  
304 available and well-studied objects; mutations like CNVs and other structural variations are  
305 experimentally confirmed [33].

306  
307 The use of cancer cell lines is advantageous due to the fact that the reviewed callers have to perform  
308 on real sequencing data, and the result can be compared to known CNVs. Using cancer cell lines can  
309 also be a disadvantage because of the lower heterogeneity found in them; high heterogeneity is a  
310 common characteristic of cancerous clinical samples. Further, variance and grades of deletions and  
311 amplifications are lowered, since a cancer cell line contains only a limited number of cells, compared  
312 to a bulk-sequenced clinical sample containing million of cells. Despite the disadvantages, testing a  
313 copy number caller's accurateness on cell lines is easy, transparent, and replicable.

314  
315 The cancer cell lines HCC1187 (with matched blood sample), HCC2218 (with matched blood sample),  
316 MCF7, PC3, and SKBR3 (Table 1) were chosen to compare MetaCNV's accurateness with other

317 callers' accurateness. The sequenced DNA of a single cell of SKBR3 (1x per cell) by using a novel  
318 method to sequence both, genome and transcriptome of the same single cell [4], was used as low  
319 coverage data. The sequenced and aligned single cell genomes were stepwise merged to present  
320 increasing coverages.

## 321 **Simulated mutated genomes**

322 For each of four coverages (1x, 2x, 5x, and 10x), three mutated human genomes were simulated (gw1,  
323 gw2, lcd). The paired-end reads for the chromosomes 1-22 were generated using CNVsim v0.9.2,  
324 aligned using Bowtie2 v2.2.9 (Langmead *et al.*, 2009), and converted, sorted and indexed using  
325 Samtools v1.2 (Li, 2011). For each of the three genomes, 30 to 50 segments per chromosome and  
326 each segment with a copy number unequal to 2 and a length of 10 kbp to 100 kbp were generated. The  
327 simulated genomes were mapped to GRCh38 (Table 2). Two simulated genomes (gw1, gw2) were  
328 used to compare the callers' results for a genome wide copy number prediction. CNVnator and  
329 Control-FREEC only gave partial predictions, see Table S4. The third simulated genome (lcd) was  
330 therefore used to compare the callers' results on a reduced data set comprising segments for which a  
331 prediction of all callers (MetaCNV, SVDetect, CNVnator, ReadDepth, Control-FREEC) was  
332 available. This, however, limited the range of copy numbers from 0 to 4.

## 333 **Results**

334 The consensus copy number caller presented here, MetaCNV, combines a number of primary callers  
335 by rules that optimally harness the strengths of each method. MetaCNV's and other callers'  
336 accurateness were evaluated by calling copy numbers for cancer cell lines and comparing the results  
337 with experimentally confirmed deleted or amplified genes in the COSMIC database. To consider a  
338 higher number of mutated genes and a wider range of copy numbers, MetaCNV's and the other  
339 callers' accurateness was also evaluated on three simulated mutated human genomes for each of the  
340 coverages 1x, 2x, 5x, and 10x.

341

342 True and predicted absolute copy numbers were compared by the mean log ratio error (MLRE) across  
343 all genes. We also calculated Matthew's correlation coefficient, MCC, on the predicted classes of  
344 deleted and amplified genes. This measure evaluates how well callers can differentiate between  
345 amplifications and deletions in general.

### 346 **Prediction accurateness on low coverage data**

347 We assessed copy number prediction accurateness on a single-cell sequenced cancer cell line (SKBR3)  
348 with stepwise merged alignments of one additional cell, and stepwise increased coverage from 1x to  
349 6x. MetaCNV was compared to the popular copy number callers CNVnator, Control-FREEC,  
350 ReadDepth, and SVDetect. In all benchmarks, MetaCNV was the most accurate method. MetaCNV  
351 outperformed the other methods in the majority of coverages in the MLRE benchmark. In all MCC  
352 benchmarks, MetaCNV was the most accurate method. MetaCNV was the most robust method as it  
353 was the top performer for MLRE, MSE, MAE, and MCC in the majority of the coverage levels  
354 (Figures 4, S13- S15, Tables S8-S10).

355  
356 CNVnator produced only a reliable classification of segments into deletions and amplifications;  
357 absolute copy numbers were not usable. For example for the SKBR3 cell line, sequenced single cell  
358 nr. 1, copy numbers for regions of deletions ranged from 0 to 2,664 and copy numbers for regions of  
359 amplifications ranged from 0 to 44,084 (Figure S8). Increasing coverage from 1x to 6x improved the  
360 accurateness only for Control-FREEC, a coverage based approach, although it never reached the  
361 accurateness of its competitors.

### 362 **Prediction accurateness on high coverage data**

363 MetaCNV's accurateness on cancer cell lines with high read coverage was compared to the  
364 accurateness of other callers which are CNVnator, CopyCat, Control-FREEC, ReadDepth, and  
365 SVDetect.

366

367 Although MetaCNV was designed for low coverage data, it also performed well for high coverage  
368 data. In three of four tested cancer cell lines, it was the best performer (Figure 5). Several predictors  
369 reached an MCC near 1.0 in two cell lines, hence there was no clear winner there. To present an  
370 overall accurateness, MLRE and MCC were averaged over the four tested cancer cell lines per caller  
371 (Figures 5c & 5d). MetaCNV showed the best overall accurateness with MLRE and second best with  
372 MCC, only 0,004 behind CNVnator.

### 373 **Prediction accurateness on simulated mutated genomes**

374 MetaCNV's predictive accurateness on simulated mutated human genomes was compared to the  
375 predictive accurateness of CNVnator, SVDetect, ReadDepth, and Control-FREEC. The simulated  
376 datasets comprise the predictions genome-wide and reduced to genes for which an output from all  
377 callers was available. Each dataset was simulated in different coverages (1x, 2x, 5x, 10x). MetaCNV  
378 performed best in all tested simulated datasets using MLRE and MCC (Figures S16A, S17, and 18A);  
379 in two datasets (2x-gw2 and 5x-lcd) MetaCNV and ReadDepth performed equally well using MLRE.

380

### 381 **The novel simNull alignment as matched sample**

382 SVDetect, one of the current input callers for MetaCNV, requires a matched sample for copy number  
383 calling. For the cancer cell lines HCC1187 and HCC2218, a matched normal blood sample was used  
384 (HCC1187BL, HCC2218BL). Additionally, a normal sample was simulated with constant coverage.  
385 However, a simulated normal sample also contains noise and variance in coverage which negatively  
386 influences copy number calling for low coverage data. Further, comparing a low coverage sample (e.g.  
387 3x) with a matched sample having higher coverage (e.g. 30x) will lead to an insensitive result.  
388 Therefore, we developed the novel idea of a simulated null alignment containing zero coverage, and  
389 thus no noise, to improve the sensitivity of copy number calling.

390

391 SVDetect using a simulated null alignment creates one of the inputs for MetaCNV. For comparison,  
392 MetaCNV was also run with input from SVDetect using a simulated normal sample. MetaCNV with a  
393 simulated null alignment achieved better overall results than with the simulated normal alignment  
394 when evaluated using MSE and MLRE (Figure S19). This was true for both low and high coverage  
395 data, although the effect was much stronger for low coverage data.

396  
397 However, just replacing the matched simulated normal sample with a simulated null alignment in  
398 SVDetect did not always improve the prediction for high coverage data, see Figure S19.

399 Taken together, the superior accurateness of MetaCNV stems from: (i) combining the prediction of  
400 multiple callers to form a consensus, (ii) considering that the reliability of a copy number depends on  
401 the approach the caller was based on, and (iii) for low coverage data, using a matched sample with  
402 zero instead of normal coverage.

## 403 **Discussion and conclusions**

404 To investigate smaller areas within a tissue section or even sequenced single cells, callers are needed  
405 that are able to detect CNVs in low coverage alignments. We present MetaCNV a copy number caller  
406 specialised in low coverage data. MetaCNV is based on a consensus approach combining different  
407 calling approaches and achieved a better prediction accurateness on low coverage data than other  
408 reviewed callers. MetaCNV also performed well on high coverage data. (Figures 4 & 5)

409  
410 In low coverage data, we observed that a read depth approach is better in predicting deleted segments,  
411 whereas amplifications were more accurately predicted by representatives of the paired-end mapping  
412 or hybrid approach. However, current callers, including those that employ a hybrid model, apply the  
413 developed calling model to each type of variation (deletions and amplifications). MetaCNV considers  
414 several calling approaches and builds a consensus based on rules to avoid overfitting, which results in  
415 predicting CN more accurately. Due to the different approaches of the current input callers

416 (ReadDepth, SVDetect, and CNVnator), MetaCNV is biased towards mid-sized and large deletions  
417 and short and mid-sized amplifications.

418

419 To identify somatic structural variants, callers such as SVDetect require a matched normal sample. In  
420 order to increase sensitivity for low coverage data, we developed the novel idea of a simulated null  
421 alignment used as matched sample. MetaCNV requires the calling result from SVDetect using this  
422 simNull as matched sample. For demonstration, MetaCNV was also tested with the input from  
423 SVDetect using a simulated normal, however, with a simNull performing a better prediction. The  
424 effect of a simulated null alignment compared with a simulated normal or matched normal is low if  
425 applied on high coverage data. In contrast, the impact increased immensely for low coverage data  
426 where, on the one hand, additional noise disturbs the prediction accurateness, and on the other hand,  
427 high sensitivity is required to predict reliable copy numbers. The simNull alignment leads to a  
428 distortion of predicted copy numbers that increases with the copy number. This distortion is corrected  
429 in a simple way, but with more alignments having different read coverages, a more sophisticated  
430 approach could lead to a further improvement in prediction.

431

432 The evaluation in this study was done using an error benchmark comparing true and predicted value  
433 per instance (gene), the mean log ratio error (MLRE), and Matthew's correlation coefficient (MCC) to  
434 assess how well a caller can distinguish between deletions and amplifications. The benchmarks mirror  
435 that coverage-based approaches are highly dependent on read coverage, and show that MetaCNV  
436 outperforms other callers on low coverage data and performs well on high coverage data.

437

438 It was not possible to include specialized low coverage scDNA callers in the benchmark. Ginkgo and  
439 SCNV can not be run for single samples and Lumpy does not output quantitative CNV values. [CNV-  
440 seq v0.2-8 gave ambiguous copy numbers for overlapping bins](#). We could however run Ginkgo using  
441 all SKBR3 single cell samples, which gives it considerably more information than the callers

442 presented in the benchmark have. Despite this, Ginkgo achieved worse accurateness than MetaCNV  
443 for all six SKBR3 cells when evaluated with MCC, and worse or equal accurateness for four cells  
444 when evaluated with MLRE.

## 445 **Availability and requirements**

446 Project name: MetaCNV  
447 Project home page: <https://bitbucket.org/sonnhammergroup/metacnv>  
448 Operating system(s): unix  
449 Programming language: C++  
450 Other requirements: GTK+-2.0 or higher  
451 Licence: GNU LGPL  
452 Any restrictions to use by non-academics: none

## 453 **List of abbreviations**

454 CNV: Copy number variation  
455 MCC: Matthew's correlation coefficient  
456 MSE: Mean squared error  
457 MAE: Mean absolute error  
458 MLRE: Mean log ratio error

## 459 **Declarations**

460 Ethics approval and consent to participate: Not applicable  
461 Consent for publication: Not applicable  
462 Availability of data and materials: All data generated or analysed during this study are included in this  
463 published article and its supplementary information files.  
464 Competing interests: The authors declare that they have no competing interests.  
465 Funding: This work was supported by AstraZeneca AB project N1372.

466 Authors' contributions: SF and ES conceptualised and designed the project, performed the data  
467 analysis and wrote the manuscript. RB and SF developed the code. All authors read and approved the  
468 final manuscript.

469 Acknowledgements: Not applicable

## 470 **References**

- 471 1. Zarrei M, MacDonald JR, Merico D, Scherer SW. A copy number variation map of the human  
472 genome. *Nat Rev Genet.* 2015;16:172–83. doi:10.1038/nrg3871.
- 473 2. Illumina. TruSeq DNA PCR-Free. 2017. [https://www.illumina.com/library-prep-array-kit-](https://www.illumina.com/library-prep-array-kit-selector.html%0A)  
474 [selector.html%0A](https://www.illumina.com/library-prep-array-kit-selector.html%0A).
- 475 3. Bock C, Farlik M, Sheffield NC. Multi-Omics of Single Cells: Strategies and Applications. *Trends*  
476 *Biotechnol.* 2016;34:605–8. doi:10.1016/j.tibtech.2016.04.004.
- 477 4. Dey SS, Kester L, Spanjaard B, Bienko M, van Oudenaarden A. Integrated genome and  
478 transcriptome sequencing of the same cell. *Nat Biotechnol.* 2015;33:285–9. doi:10.1038/nbt.3129.
- 479 5. Mills RE, Walter K, Stewart C, Handsaker RE, Chen K, Alkan C, et al. Mapping copy number  
480 variation by population-scale genome sequencing. *Nature.* 2011;470 July 2010:59–65.  
481 doi:10.1038/nature09708.Mapping.
- 482 6. Zhao M, Wang Q, Wang Q, Jia P, Zhao Z. Computational tools for copy number variation (CNV)  
483 detection using next-generation sequencing data: Features and perspectives. *BMC Bioinformatics.*  
484 2013;14:S1. doi:10.1186/1471-2105-14-S11-S1.
- 485 7. Miller CA, Hampton O, Coarfa C, Milosavljevic A. ReadDepth: A parallel R package for detecting  
486 copy number alterations from short sequencing reads. *PLoS One.* 2011;6:e16327.  
487 doi:10.1371/journal.pone.0016327.
- 488 8. Xie C, Tammi MT. CNV-seq, a new method to detect copy number variation using high-throughput  
489 sequencing. *BMC Bioinformatics.* 2009;10:1–9.
- 490 9. Klambauer G, Schwarzbauer K, Mayr A, Clevert DA, Mitterecker A, Bodenhofer U, et al.  
491 Cn.MOPS: Mixture of Poissons for discovering copy number variations in next-generation

- 492 sequencing data with a low false discovery rate. *Nucleic Acids Res.* 2012;40:e69.  
493 doi:10.1093/nar/gks003.
- 494 10. Boeva V, Popova T, Bleakley K, Chiche P, Cappo J, Schleiermacher G, et al. Control-FREEC: A  
495 tool for assessing copy number and allelic content using next-generation sequencing data.  
496 *Bioinformatics.* 2012;28:423–5. doi:10.1093/bioinformatics/btr670.
- 497 11. Abyzov A, Urban AE, Snyder M, Gerstein M. CNVnator: An approach to discover, genotype, and  
498 characterize typical and atypical CNVs from family and population genome sequencing. *Genome*  
499 *Res.* 2011.
- 500 12. Medvedev P, Stanciu M, Brudno M. Computational methods for discovering structural variation  
501 with next-generation sequencing. *Nat Methods.* 2009.
- 502 13. Alkan C, Coe BP, Eichler EE. Genome structural variation discovery and genotyping. *Nature*  
503 *Reviews Genetics.* 2011.
- 504 14. Chen K, Wallis JW, McLellan MD, Larson DE, Kalicki JM, Pohl CS, et al. BreakDancer: An  
505 algorithm for high-resolution mapping of genomic structural variation. *Nat Methods.* 2009;6:677–  
506 81. doi:10.1038/nmeth.1363.
- 507 15. Ye K, Schulz MH, Long Q, Apweiler R, Ning Z. Pindel: A pattern growth approach to detect  
508 break points of large deletions and medium sized insertions from paired-end short reads.  
509 *Bioinformatics.* 2009;25:2865–71.
- 510 16. Zeitouni B, Boeva V, Janoueix-Lerosey I, Loeillet S, Legoix-né P, Nicolas A, et al. SVDetect: A  
511 tool to identify genomic structural variations from paired-end and mate-pair sequencing data.  
512 *Bioinformatics.* 2010;26:1895–6. doi:10.1093/bioinformatics/btq293.
- 513 17. Medvedev P, Fiume M, Dzamba M, Smith T, Brudno M. Detecting copy number variation with  
514 mated short reads. *Genome Res.* 2010.
- 515 18. Garvin T, Aboukhalil R, Kendall J, Baslan T, Atwal GS, Hicks J, et al. Interactive analysis and  
516 assessment of single-cell copy-number variations. *Nature Methods.* 2015;12:1058–60.

- 517 19. Wang X, Chen H, Zhang NR. DNA copy number profiling using single-cell sequencing. *Brief*  
518 *Bioinform.* 2018.
- 519 20. Layer RM, Chiang C, Quinlan AR, Hall IM. LUMPY: A probabilistic framework for structural  
520 variant discovery. *Genome Biol.* 2014.
- 521 21. Meier-Kolthoff JP, Auch AF, Huson DH, Goker M. COPYCAT : cophylogenetic analysis tool.  
522 *Bioinformatics.* 2007;23:898–900. doi:10.1093/bioinformatics/btm027.
- 523 22. Gibbs RA, Boerwinkle E, Doddapaneni H, Han Y, Korchina V, Kovar C, et al. A global reference  
524 for human genetic variation. *Nature.* 2015;526:68–74. doi:10.1038/nature15393.
- 525 23. Hu X, Yuan J, Shi Y, Lu J, Liu B, Li Z, et al. pIRS: Profile-based illumina pair-end reads  
526 simulator. *Bioinformatics.* 2012;28:1533–5. doi:10.1093/bioinformatics/bts187.
- 527 24. Eisfeldt J, Nilsson D, Andersson-Assarsson JC, Lindstrand A. AMYCNE: Confident copy number  
528 assessment using whole genome sequencing data. *PLoS One.* 2018;13:e0189710.  
529 doi:10.1371/journal.pone.0189710.
- 530 25. Legault MA, Girard S, Perreault LPL, Rouleau GA, Dubé MP. Comparison of sequencing based  
531 CNV discovery methods using monozygotic twin quartets. *PLoS One.* 2015.
- 532 26. Duan J, Zhang J-GJ-G, Deng H-WH-W, Wang Y-PY-P. Comparative Studies of Copy Number  
533 Variation Detection Methods for Next-Generation Sequencing Technologies. *PLoS One.*  
534 2013;8:59128. doi:10.1371/journal.pone.0059128.
- 535 27. Wang R, Lin D, Jiang Y. SCOPE: A normalization and copy number estimation method for  
536 single-cell DNA sequencing. 2019.
- 537 28. Wackerly D, Mendenhall W, Scheaffer RL. *Mathematical Statistics with Applications.* 2008.  
538 Accessed 24 Aug 2019.
- 539 29. Matthews BW. Comparison of the predicted and observed secondary structure of T4 phage  
540 lysozyme. *BBA - Protein Struct.* 1975.
- 541 30. Zerbino DR, Achuthan P, Akanni W, Amode MR, Barrell D, Bhai J, et al. Ensembl 2018. *Nucleic*  
542 *Acids Res.* 2018.

543 31. Forbes SA, Beare D, Boutselakis H, Bamford S, Bindal N, Tate J, et al. COSMIC: Somatic cancer  
544 genetics at high-resolution. *Nucleic Acids Res.* 2017;45:D777–83. doi:10.1093/nar/gkw1121.

545 32. Landry JJM, Pyl PT, Rausch T, Zichner T, Tekkedil MM, Stütz AM, et al. The Genomic and  
546 Transcriptomic Landscape of a HeLa Cell Line supplement. *G3 Genes|Genomes|Genetics.*  
547 2013;3:1213–24. doi:10.1534/g3.113.005777.

548 33. Masters JRW. Human cancer cell lines: fact and fantasy. *Nat Rev Mol Cell Biol.* 2000;1:233–6.  
549 doi:10.1038/35043102.

550 34. Greenman CD, Bignell G, Butler A, Edkins S, Hinton J, Beare D, et al. PICNIC: An algorithm to  
551 predict absolute allelic copy number variation with microarray cancer data. *Biostatistics.*  
552 2010;11:164–75. doi:10.1093/biostatistics/kxp045.

553 35. Berglund E, Maaskola J, Schultz N, Friedrich S, Marklund M, Bergenstråhle J, et al. Spatial maps  
554 of prostate cancer transcriptomes reveal an unexplored landscape of heterogeneity. *Nat Commun.*  
555 2018;9.

556 36. Langmead B, Trapnell C, Pop M, Salzberg SL. Ultrafast and memory-efficient alignment of short  
557 DNA sequences to the human genome. *Genome Biol.* 2009;10:R25. doi:10.1186/gb-2009-10-3-  
558 r25.

559 37. Broad Institute. Picard tools. <https://broadinstitute.github.io/picard/>. 2016.

560 38. Li H. A statistical framework for SNP calling, mutation discovery, association mapping and  
561 population genetical parameter estimation from sequencing data. *Bioinformatics.* 2011;27:2987–  
562 93. doi:10.1093/bioinformatics/btr509.

563

564 **Table 1.** Cancer cell lines used for accurateness testing. Coverage and number of deleted and  
565 amplified genes extracted from COSMIC are presented. Copy numbers were called from sequenced  
566 genomes and experimentally confirmed with PICNIC [34].

Cancer	Coverage	# of amplified	# of deleted	Total # of	Ratio
--------	----------	----------------	--------------	------------	-------

cell line		genes	genes	genes with CNVs	amplified/ deleted genes
HCC1187	104x	154	46	200	3.48
HCC2218	93x	200	36	236	5.55
MCF7	62x	49	30	79	1.63
PC3	76x	179	222	401	0.81
Single-cell SKBR3	6 stepwise merged single cells with 1x to 6x	161	29	190	5.55

567

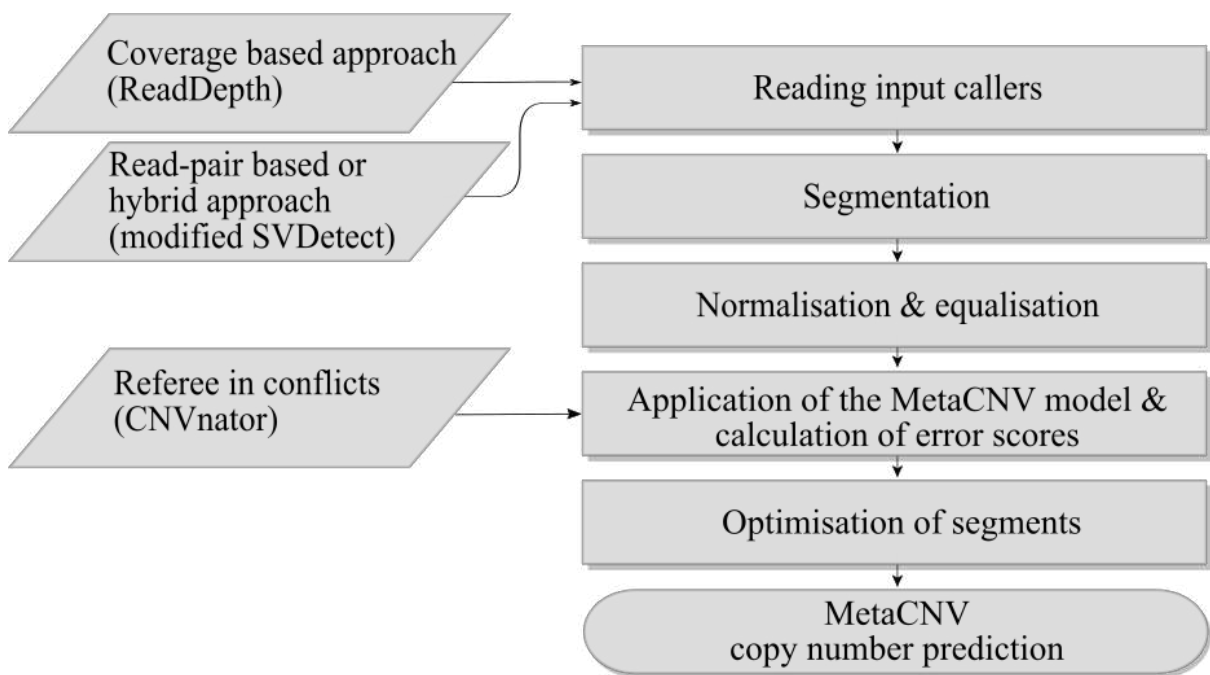
568 Table 2. Simulated mutated genomes used for accurateness testing. The simulated data sets gw1 and  
569 gw2 were used to compare the prediction results for a genome-wide prediction. The simulated data  
570 sets lcd was used to compare the prediction results for genes for which a prediction of all tested caller  
571 was available.

Simulation	Depth of coverage	# of amplified genes	# of deleted genes	Total # of genes	Ratio amplified/ deleted genes
sim 1x gw1	1.1x	283	559	13906	0.51
sim 1x gw2	1.1x	236	573	13920	0.41
sim 1x lcd	1.5x	25	30	330	0.83
sim 2x gw1	2.2x	247	560	13937	0.44
sim 2x gw2	2.2x	254	588	13922	0.43
sim 2x lcd	2.9x	42	44	16	0.95

sim 5x gw1	5.7x	230	580	13987	0.40
sim 5x gw2	5.7x	251	593	13949	0.42
sim 5x lcd	7.3x	62	48	14	1.29
sim 10x gw1	11.3x	263	560	13882	0.47
sim 10x gw2	11.3x	240	551	13865	0.44
sim 10x lcd	14.9x	54	49	7	1.10

572

573

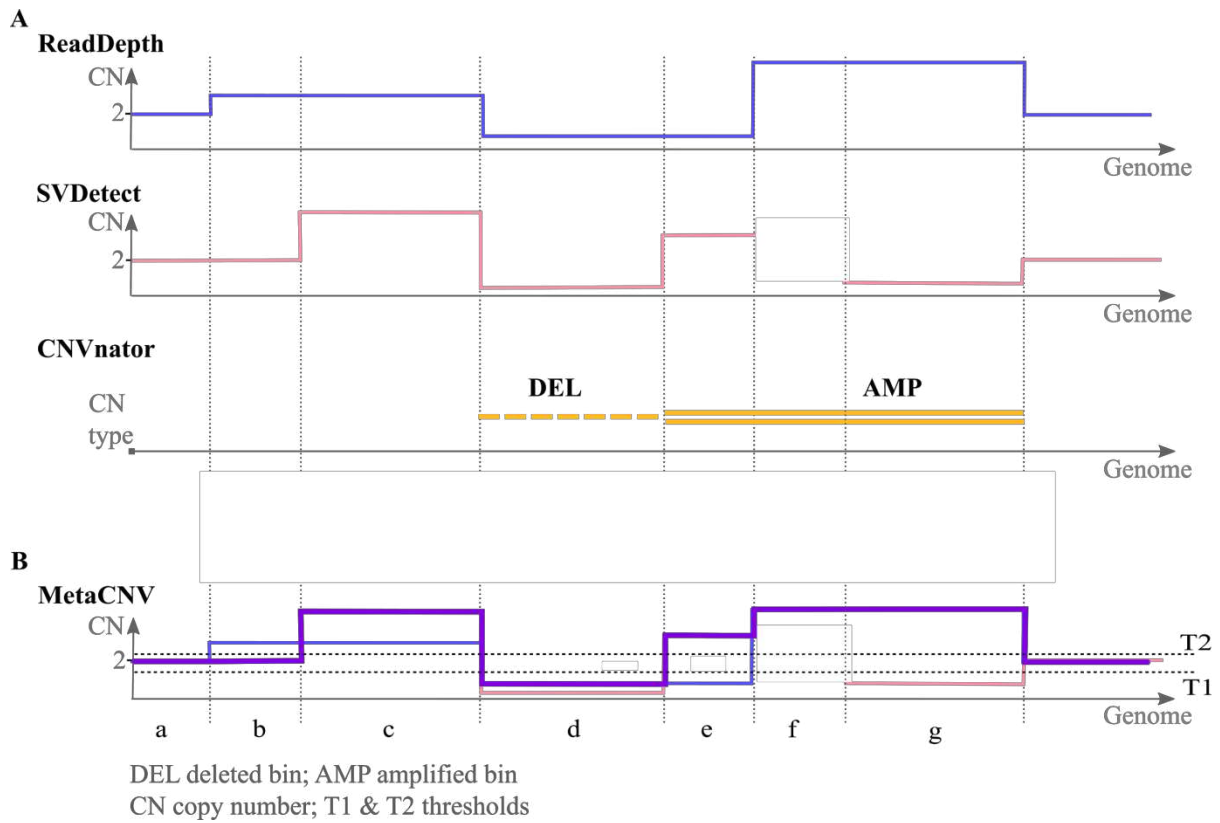


574

575 **Figure 1.** MetaCNV workflow to call copy numbers. MetaCNV requires as input an SVDetect

576 prediction using a simulated null alignment (simNull) as matched sample (Figure S19).

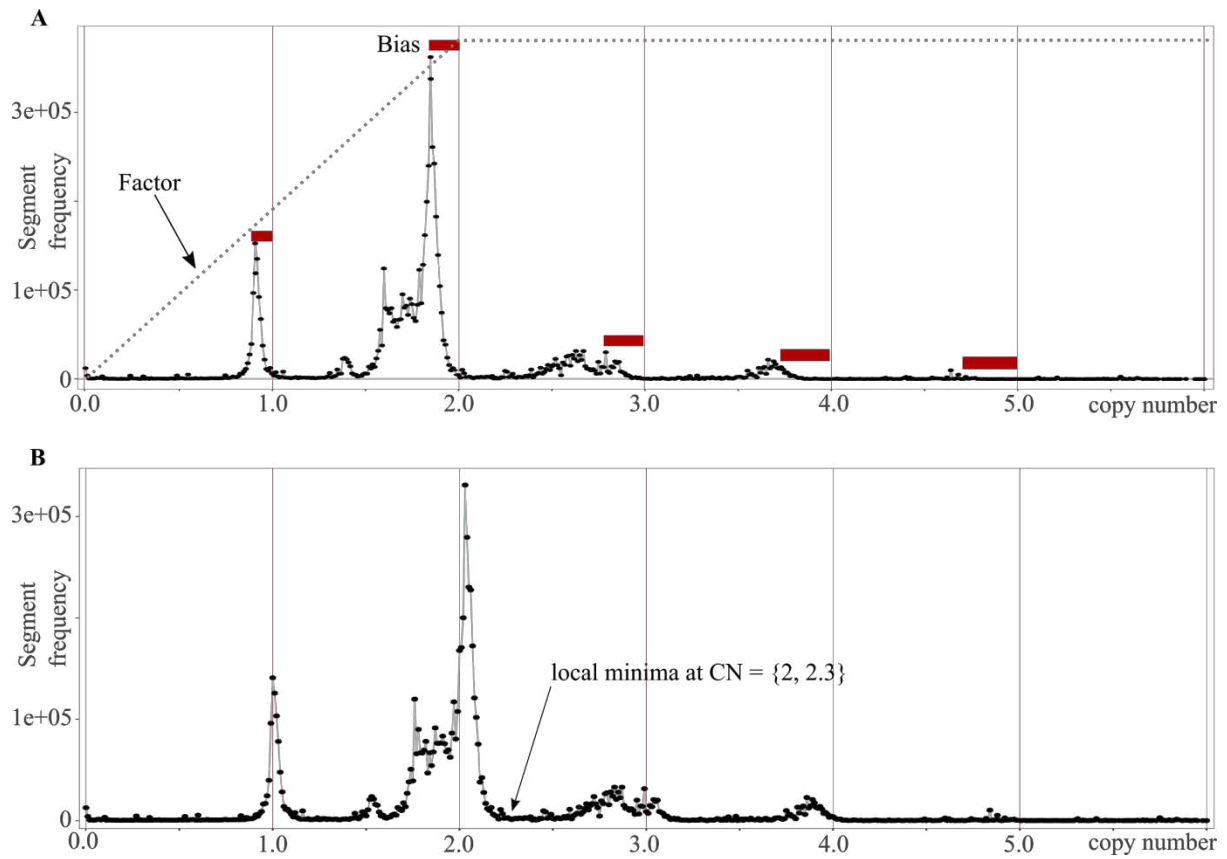
577



578

579 **Figure 2.** Genome segmentation by MetaCNV. **A.** Segmentation of the genome according to the bins  
 580 and breakpoints from the input callers. **B.** Consensus segment prediction by MetaCNV is marked as a  
 581 thick line. Bins c is predicted as amplified and bin d as deleted. Here there is no conflict between the  
 582 input callers, hence the consensus is that c is amplified and d is deleted. Bin f is not predicted by  
 583 SVDetect, but because ReadDepth predicts it as an amplification, this becomes the consensus. Bins b,  
 584 e and g have conflicting ReadDepth and SVDetect predictions. CNVnator judges that e and g are  
 585 amplifications, hence this becomes the consensus. Bin b is set to CN 2 because only ReadDepth  
 586 predicts it as an amplification and CNVnator makes no prediction (Table S18).

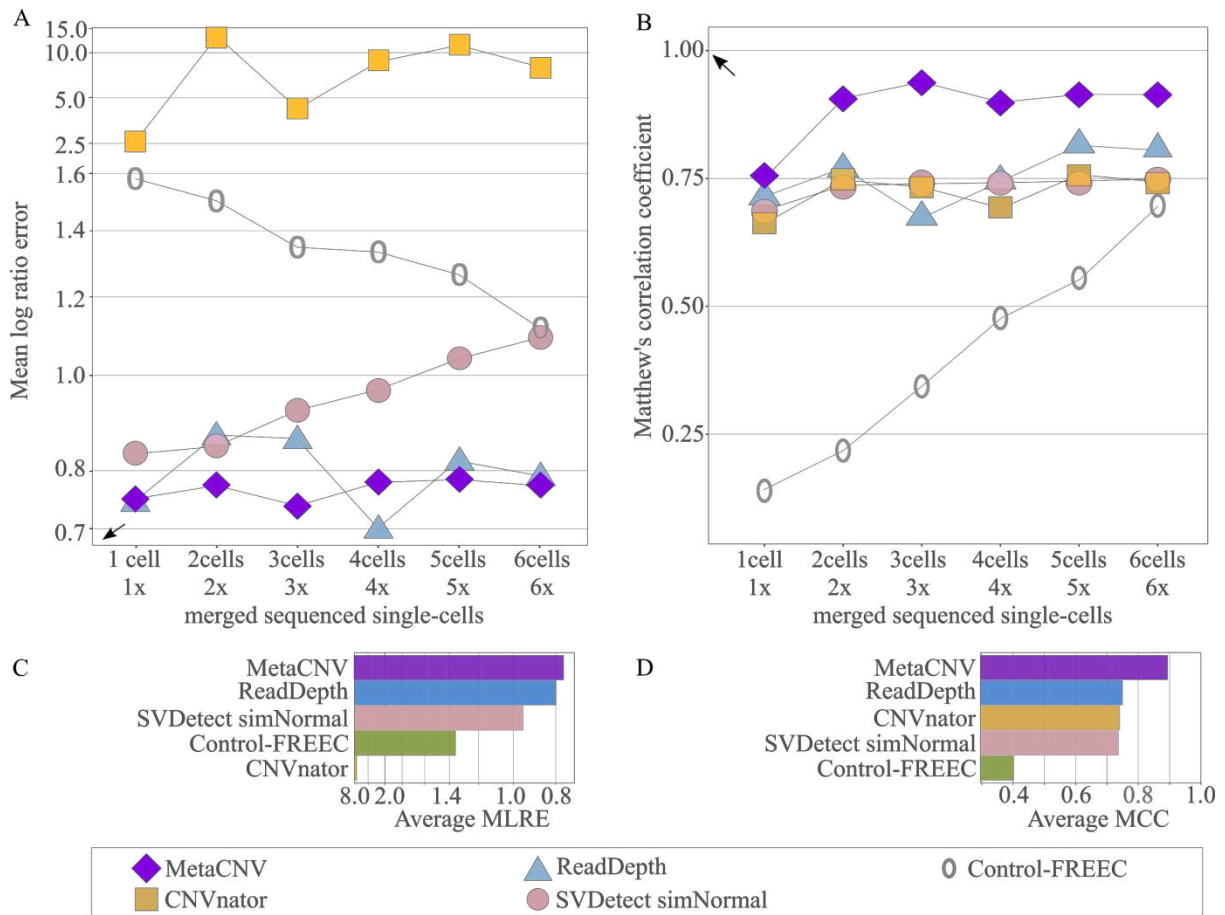
587



588

589 **Figure 3.** Distribution of absolute copy numbers. Copy numbers were called with ReadDepth of  
 590 cancer cell line HCC2218 after segmentation (6,867,679 segments with an average segment length of  
 591 450 bp). **A.** The bias occurs around each integer copy number and is lower for  $CN_{RD} \sim 1$ , but increases  
 592 for  $CN_{RD} \sim 2$ . The factor for normalisation is a linear function (equation 1b) which serves to adjust the  
 593 bias for different  $CN_{RD}$ . **B.** Distribution of absolute copy numbers called with ReadDepth after  
 594 normalisation

595



596

597

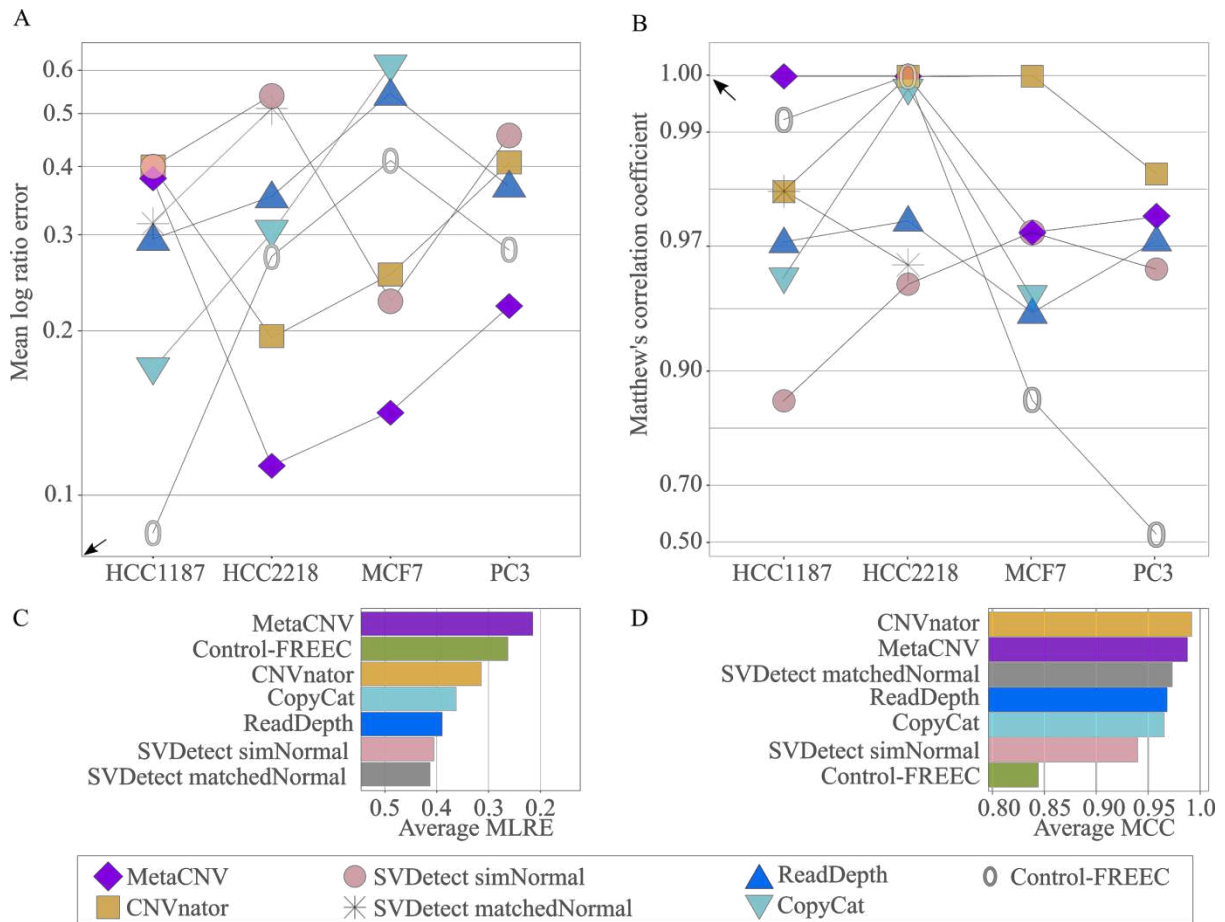
598

599

600

601

**Figure 4.** Prediction accurateness of MetaCNV on low coverage data, compared to CNVnator, Control-FREEC, ReadDepth, and SVDetect. **A** and **B** present the benchmark results with MLRE and MCC per merged alignment. **C** and **D** show the overall results averaged across all benchmarked alignments.



602

603

**Figure 5.** Prediction accurateness of MetaCNV and other copy number callers for high coverage data.

604

**A** and **B** present the average benchmark results per cancer cell line. SVDetect using matchedNormal

605

could only be performed for HCC1187 and HCC2218, for which matched blood samples were

606

available. **C** and **D** show the overall results averaged across all benchmarked cell lines.

607

### Electronic supplementary material

File name	Description of data
Additional file 1	Supplementary methods, figures and tables (DOCX)
Additional file 2	MetaCNV Readme (manual to run MetaCNV, TXT)
Additional file 3	Supplementary table containing genes per cancer cell line, incl. Copy number, segment length and evaluation length (XLS).

608

## Figures

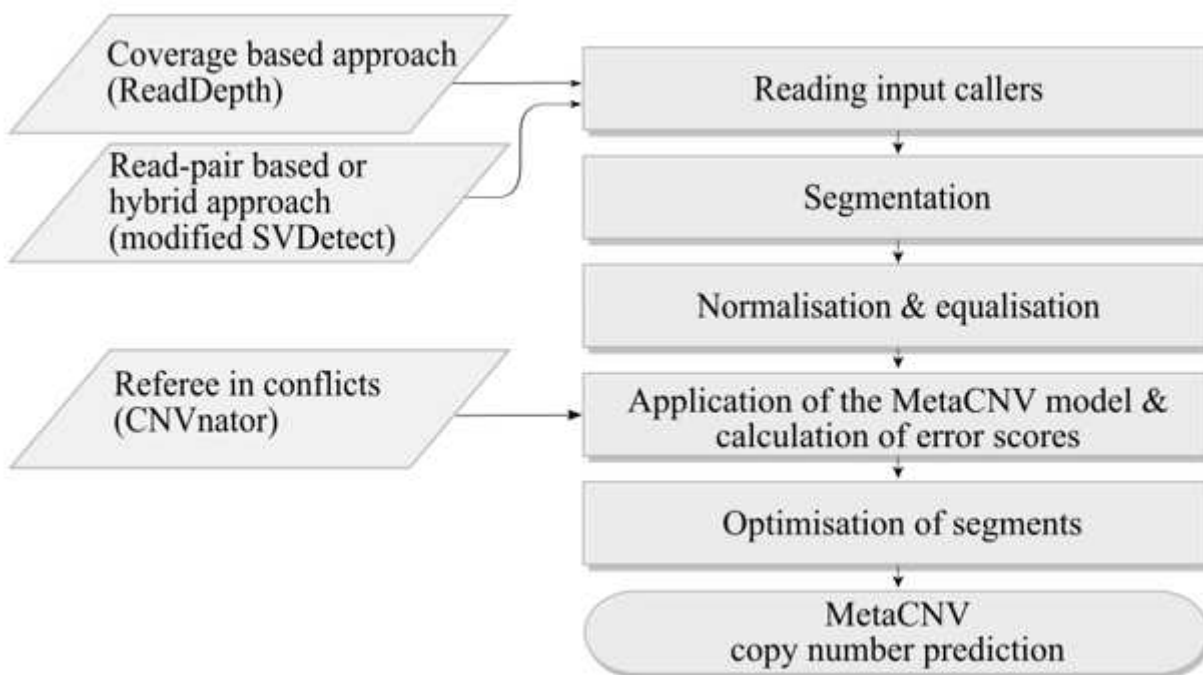


**Figure 1**

MetaCNV workflow to call copy numbers. MetaCNV requires as input an SVDetect prediction using a simulated null alignment (simNull) as matched sample (Figure S19).

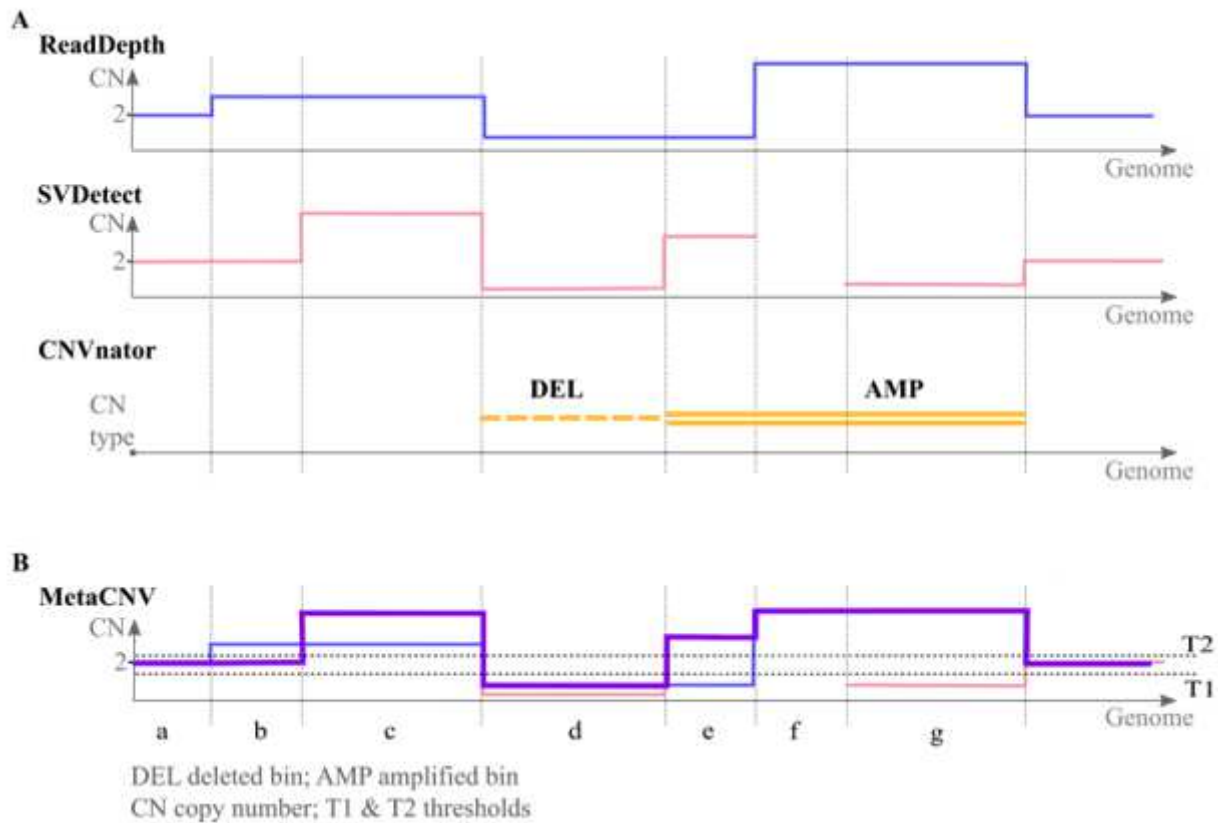


**Figure 2**

Genome segmentation by MetaCNV. A. Segmentation of the genome according to the bins and breakpoints from the input callers. B. Consensus segment prediction by MetaCNV is marked as a thick line. Bins c is predicted as amplified and bin d as deleted. Here there is no conflict between the input callers, hence the consensus is that c is amplified and d is deleted. Bin f is not predicted by SVDetect, but because ReadDepth predicts it as an amplification, this becomes the consensus. Bins b, e and g have conflicting ReadDepth and SVDetect predictions. CNVnator judges that e and g are amplifications, hence this becomes the consensus. Bin b is set to CN 2 because only ReadDepth predicts it as an amplification and CNVnator makes no prediction (Table S18).

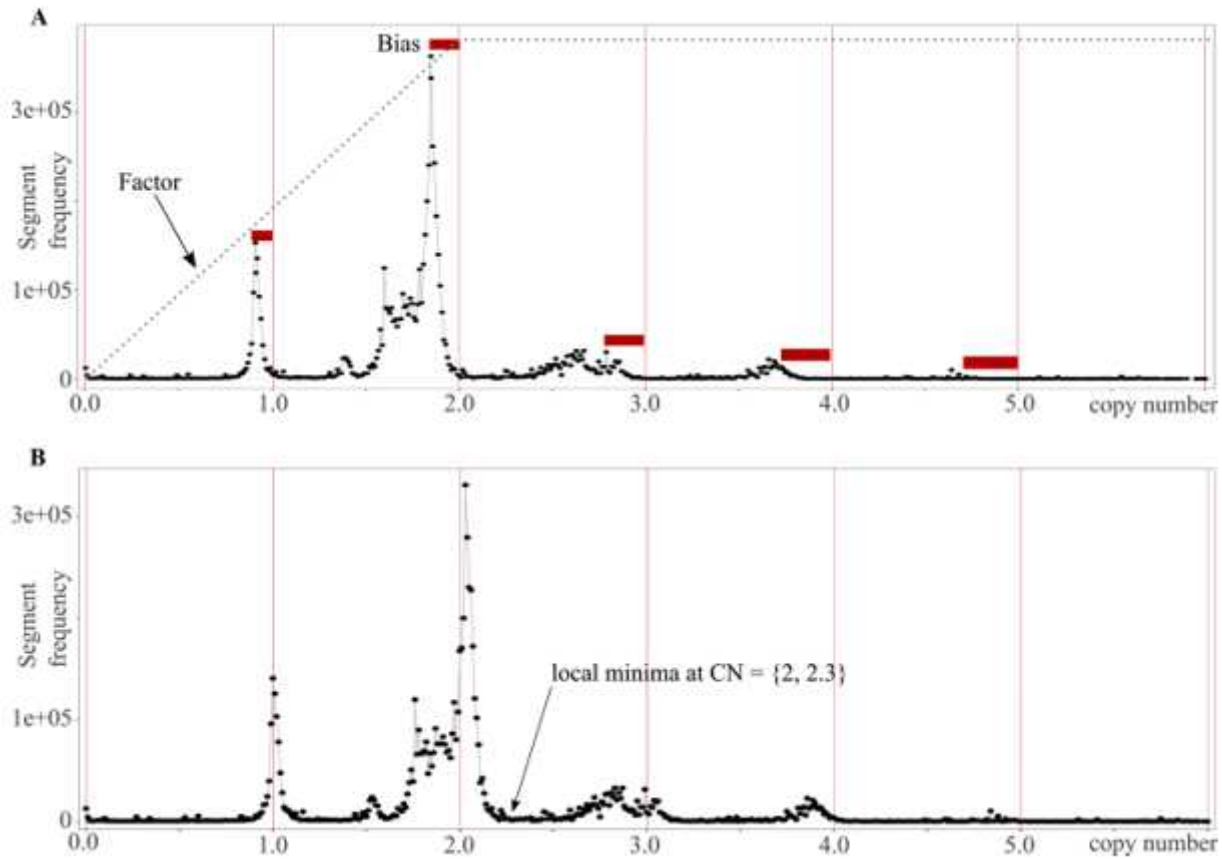


**Figure 3**

Distribution of absolute copy numbers. Copy numbers were called with ReadDepth of cancer cell line HCC2218 after segmentation (6,867,679 segments with an average segment length of 450 bp). A. The bias occurs around each integer copy number and is lower for CNRD  $\sim 1$ , but increases for CNRD  $\sim 2$ . The factor for normalisation is a linear function (equation 1b) which serves to adjust the bias for different CNRD. B. Distribution of absolute copy numbers called with ReadDepth after normalisation

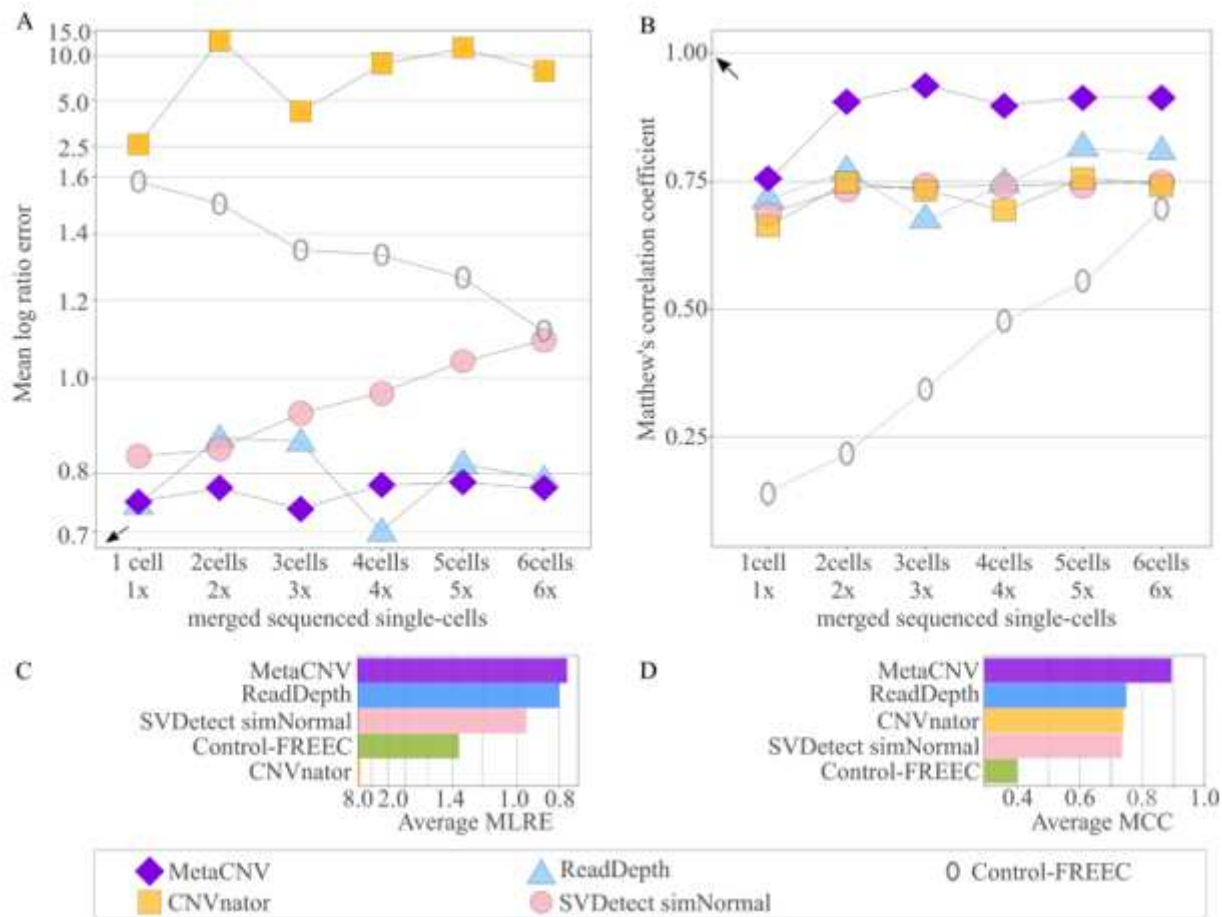


**Figure 4**

Prediction accurateness of MetaCNV on low coverage data, compared to CNVnator, Control-FREEC, ReadDepth, and SVDetect. A and B present the benchmark results with MLRE and MCC per merged alignment. C and D show the overall results averaged across all benchmarked alignments.

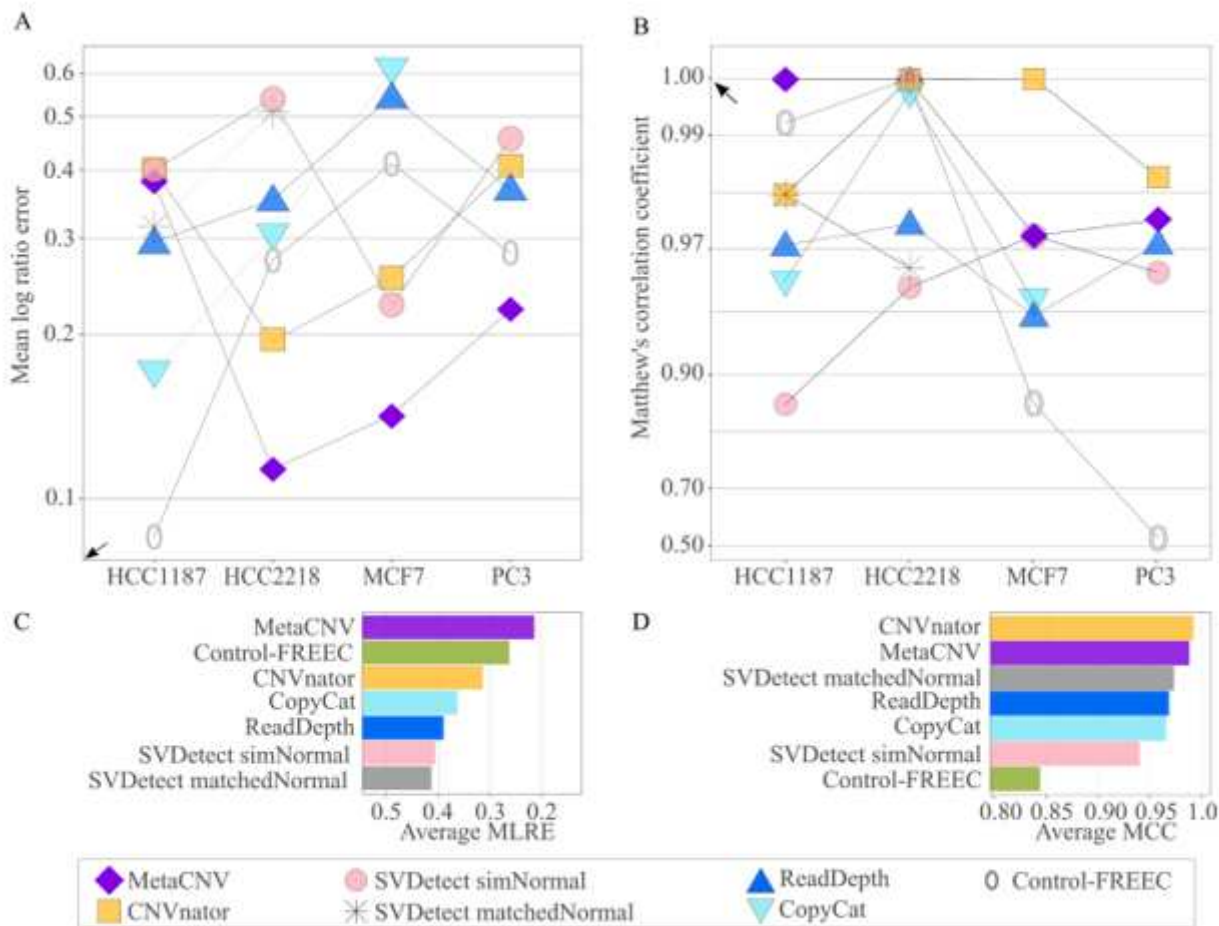


**Figure 5**

Prediction accurateness of MetaCNV and other copy number callers for high coverage data. A and B present the average benchmark results per cancer cell line. SVDetect using matchedNormal could only be performed for HCC1187 and HCC2218, for which matched blood samples were available. C and D show the overall results averaged across all benchmarked cell lines.

## Supplementary Files

This is a list of supplementary files associated with this preprint. Click to download.

- [metaCNVsupplementv2reSubmission.docx](#)
- [CCLknownCNVs.xlsx](#)
- [README.txt](#)